Automatic and Robust Skull Registration Based on Discrete Uniformization

Junli Zhao[1], Xin Qi[2], Chengfeng Wen[2], Na Lei*[3], and Xianfeng Gu[2]

[1]School of Data Science and Software Engineering,Qingdao University, Qingdao,China
[2]Department of Computer Science,Stony Brook University, Stony Brook,USA
[3]International School of Information Science and Engineering, Dalian University of Technology, Dalian,China

[1,2,3]zhaojl@yeah.net,xinqi@cs.stonybrook.edu,chwen@cs.stonybrook.edu,,
⋆Corresponding:nalei@dlut.edu.cn,gu@cs.stonybrook.edu

Abstract

Skull registration plays a fundamental role in forensic science and is crucial for craniofacial reconstruction. The complicated topology, lack of anatomical features, and low quality reconstructed mesh make skull registration challenging. In this work, we propose an automatic skull registration method based on the discrete uniformization theory, which can handle complicated topologies and is robust to low quality meshes. We apply dynamic Yamabe flow to realize discrete uniformization, which modifies the mesh combinatorial structure during the flow and conformally maps the multiply connected skull surface onto a planar disk with circular holes. The 3D surfaces can be registered by matching their planar images using harmonic maps. This method is rigorous with theoretic guarantee, automatic without user intervention, and robust to low mesh quality. Our experimental results demonstrate the efficiency and efficacy of the method.

1. Introduction

The skull is an intrinsic biological feature of humans. Wilkinson [39] shows that the shape of a skull determines the person's facial features, therefore the face can be reconstructed from the skull, which is called craniofacial reconstruction. With the rapid development of computer technology, computer-assisted craniofacial reconstruction plays an important role in the unknown corpse identification of criminal investigation, skull identification in forensic science, understanding of human beings evolution in anthropology, etc. Skull registration is a key pre-processing step of craniofacial reconstruction.

Surface registration is a fundamental problem in computer vision, which seeks an optimal mapping from the target data to the reference data to achieve one-to-one correspondence between them. The three-dimensional(3D) skull registration aims at finding a one-to-one correspondence between the dense points for different posed and sized 3D skull models. Establishing accurate registration of craniofacial data is the foundation and premise of building craniofacial statistical models.

In general, skull registration is challenging, because skull surfaces have very complicated topological structures, different morphology, and non-rigid deformation. Furthermore, feature definition and extraction are difficult as well. Hence conventional methods can hardly achieve automatic registration. Meshes produced by 3D scanning or reconstruction from CT images are with low qualities; this makes the numerical computation highly unstable. Although many researchers have made great efforts, automatic and robust skull registration still remains a fundamental challenge.

In order to handle complex topologies and improve the robustness for the registration, we propose a novel method based on the recent theoretic break through : discrete uniformization theory, which can handle surfaces with arbitrary topologies and poor mesh qualities. Different from the previous method, dynamic Yamabe flow is used to realize discrete uniformization. So our method is rigorous with theoretic guarantee to convergence on an arbitrary triangular mesh and achieves global diffeomorphism and high registration accuracy, which outperforms other methods.

Contributions This work proposes a novel method for skull registration. The method has some merits:

1. Rigorous: the discrete uniformization theory guarantees the existence and the uniqueness of the solution, hence the algorithm has solid theoretic foundation;

2. Automatic: the whole computational pipeline is automatic, without any manual input or user intervention;
3. Robust: the uniformization theory holds for arbitrary polygonal surfaces, therefore the algorithm is insensitive to the mesh qualities;
4. Effective: the experimental results demonstrate the effectiveness, accuracy and robustness of our method;
5. General: the method is general enough to handle surfaces with complicated topologies.

2. Related Work

The literature for registration is vast, here we only briefly review the most related 3D surface registration works.

2.1. Rigid Registration Method

The rigid registration methods use rigid transformations to match shapes. The Iterative Closest Point (ICP) proposed by Besl and McKay [2] is the most classical rigid registration method. Due to local search, ICP often falls into local optima and is sensitive to the initialization quality. There are various improved ICP methods [40, 1] proposed. Rusinkiewicz and Levoy [33] summarized various ICP variant algorithms, and improved the ICP algorithm from the following aspects: control point selection, feature metrics, spatial search, point pair weights and rigid body transformation.Cheng et al.[8] proposed a 3d skull registration method based on clifford algebra pupil distance invariability and built a corresponding visualization registration platform. Accurate point-to-point correspondence between skulls is difficult to establish by rigid registration.

2.2. Non-Rigid Registration Method

Non-rigid registration methods adopt non-rigid transformations, which can capture the deformation between different samples. Thin Plate Splines (TPS) transformation methods are popular [11, 4, 5, 23, 3]. Chui and Rangarajan [11] proposed the TPS-RPM registration method which aims to add TPS into the framework of ICP. Schneider and Eisert proposed an automatic registration method for 3D head data [34] by combining ICP and TPS. Deng et al. [13] proposed a skull registration method that combines global and local deformation. Chen et al [7] proposed a non-rigid 3D craniofacial registration method using TPS transformation and cylindrical projection. Most of these methods depend on the manually calibrated feature points which is time-consuming and subjective. Although Hu et al. [22, 32] proposed iterative TPS registration methods based on random sampling control points, the registration results can not be guaranteed.

2.3. Conformal Parameterization Method

Conformal parameterization [16, 37, 45] is a powerful tool in delivering 2D representations from 3D surfaces while preserving local features and constructing the correspondence between them. The nature of conformal mapping makes it insensitive to surface deformation and is particularly suitable for 3D non-rigid surfaces registration.

Several conformal parameterization registration methods are realized in 3D facial surface registration and show good results [41, 25, 29, 50, 36]. Many computational approaches have been introduced such as least-square conformal mapping [27, 26], holomorphic differentials based approaches [46] and Ricci flow techniques [25, 24, 45]. Koebe's iteration was generalized to compute conformal parameterization for genus zero surface with multiple boundary components [47] and high genus surfaces with boundaries in [49]. Wang [38]applied harmonic map for high resolution, non-rigid dense 3D point tracking, and Shi [35]applied it to study constrained human brain surface registration. Zeng et al. [46] have applied Hyperbolic Ricci Flow into 3D face matching and registration.

In order to handle complicated topology and large deformation, we select the conformal parameterization as the main tool for skull registration because 3D shape registration through 2D conformal parameterization greatly reduces the difficulty and improves the accuracy. Unfortunately most existing conformal parameterization methods require good mesh quality. Eventually, we choose the discrete uniformization method [17], because this method can handle surfaces with arbitrary topology and low mesh quality.

3. Theoretic Background

This section briefly introduces the theoretic background, for detailed treatments we refer readers to [30, 18, 12]. Especially, detailed proofs for discrete uniformization theorem are avalable [17] and [14].

3.1. Smooth Surface Uniformization

Uniformization theorem is one of the most fundamental theorems in differential geometry.

Theorem 1 (Poincaré-Koebe Uniformization 1907) *Suppose S is a closed surface with a Riemannian metric $\mathbf{g}$, there exists a function $u : S \to \mathbb{R}$, such that the metric $e^{2u}\mathbf{g}$ induces constant Gaussian curvature. The constant is $+1, 0, -1$ for surfaces with positive, zero and negative Euler characteristic number respectively.*

A modern proof is based on Hamilton's Ricci flow.

Definition 1 (Normalized Hamilton's Ricci flow) *Given a closed Riemannian surface (S, g), the flow equation is defined as:*

$$\frac{du(t)}{dt} = -2\left(K(t) - 2\pi\frac{\chi(S)}{A(t)}\right)$$

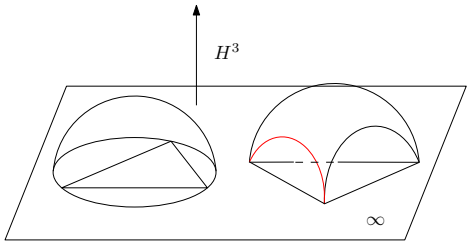

Figure 1: Hyperbolic hull of a Euclidean triangle on the plane at infinity.

where $g(t) = e^{2u(t)}g(0)$, $K(t)$ denotes the Gaussian curvature, while $\chi(S)$ and $A(t)$ represent the Euler characteristic and the total area of the surface S respectively.

The proof of convergence of Ricci flow equation [19, 20, 10] and the solution leads to the conformal uniformization metric. For registration purposes, conformal mapping has been broadly used.

Definition 2 (Conformal mapping) *Given that $(S_1, \mathbf{g}_1)$ and $(S_2, \mathbf{g}_2)$ are Riemannian surfaces with Riemannian metric $\mathbf{g}_1$ and $\mathbf{g}_2$ respectively, a smooth mapping $\phi : S_1 \to S_2$ is conformal, if the pull-back metric induced by ϕ and the original metric differ by a scalar function: $\phi^*\mathbf{g}_2 = e^{2\lambda}\mathbf{g}_1$, where $\lambda : S_1 \to \mathbb{R}$ is scalar function.*

Conformal mappings preserve angles and thus map infinitesimal circles to infinitesimal circles [18]. Multiple techniques [46, 45, 25, 6] have been introduced in the literature.

3.2. Discrete Uniformization

This work is based on discrete uniformization theory [17, 14]. The upper half space model for hyperbolic space $\mathbb{H}^3$ is assigned with a Riemannian metric $ds^2 = (dx^2 + dy^2 + dz^2)/z^2$. The geodesics are vertical lines or circular arcs orthogonal to the xy-plane. The hyperbolic planes are the semi-spheres with equators on the xy-plane. The xy-plane is the plane at infinity.

Suppose we put a Euclidean triangle Δ at the xy-plane, the hemisphere through its circumcircle is a hyperplane $\mathbb{H}^2$ (As shown in Figure 1). Through each pair of vertices, there is a hyperbolic geodesic. The three geodesics on $\mathbb{H}^2$ form a *hyperbolic ideal triangle*, which is the *hyperbolic convex hull* of the three vertices.

Suppose M is a triangular polyhedral surface, a pair of adjacent triangles Δ_1 and Δ_2, the intersection is an edge $\Delta_1 \cap \Delta_2 = e$. The two triangles are isometrically embedded on the xy-plane, the two hyperbolic convex hull are glued along the geodesic through the end vertices of e. In this way, we can glue the hyperbolic convex hulls of all faces to form a hyperbolic surface $\tilde{M}$ with cusps at the vertices.

Definition 3 (Discrete Conformal Equivalence) *Given two triangular polyhedral surfaces M_1 and M_2, if their corresponding hyperbolic surfaces $\tilde{M}_1$ and $\tilde{M}_2$ are isometric, then two polyhedral surfaces are discrete conformal equivalent, denoted as $M_1 \sim M_2$.*

The Euclidean metric on a triangle mesh induces discrete curvature. On each triangle $[v_i, v_j, v_k]$, the metric determines the corner angles. θ_i^{jk} is denoted the angle at the vertex v_i.

Definition 4 (Discrete Gaussian Curvature) *Discrete Gaussian curvature is defined as angle deficit on vertices, $K : V \to \mathbb{R}$,*

$$K(v) = \begin{cases} 2\pi - \sum_{jk} \theta_i^{jk}, & v \notin \partial M \\ \pi - \sum_{jk} \theta_i^{jk}, & v \in \partial M \end{cases} \tag{1}$$

It can be easily shown that the total discrete Gaussian curvature satisfies the discrete Gauss-Bonnet condition [18]

$$\sum_i K(v_i) = 2\pi\chi(M). \tag{2}$$

Our method is based on the following newly discovered theorem by Yau et al.[17]

Theorem 2 (Discrete Uniformization) *Given a triangular polygonal surface M, given target curvature $\bar{K} : V \to \mathbb{R}$ satisfying Gauss-Bonnet condition 2 and $\bar{K}(v_i) \in (-\infty, 2\pi]$, then there exists another polyhedral surface $\tilde{M}$ discrete conformal to M, such that the discrete Gaussian curvature of $\tilde{M}$ equals to $\bar{K}$.*

3.3. Dynamic Yamabe Flow

The discrete uniformization can be obtained by dynamic Yamabe flow. The metric g on discrete surface M is represented as edge length function, $l : E \to \mathbb{R}^+$, with triangle inequality satisfied.

Derived from finite element method, the *cotangent edge weight* for an interior edge $[v_i, v_j]$, adjacent to faces $[v_i, v_j, v_k]$ and $[v_j, v_i, v_l]$, is defined as

$$w_{ij} = \cot\theta_k^{ij} + \cot\theta_l^{ij} \tag{3}$$

Since a boundary edge $[v_i, v_j]$ is only adjacent to one face $[v_i, v_j, v_k]$, the corresponding edge weight is defined as

$$w_{ij} = \cot\theta_k^{ij} \tag{4}$$

We say a triangulation is *Delaunay* if all edge weights are non-negative.

Definition 5 *(Discrete Surface Dynamic Yamabe Flow) Discrete surface dynamic Yamabe flow is defined as*

$$\frac{du_i(t)}{dt} = \bar{K}_i - K_i(t) \tag{5}$$

where u_i is the discrete conformal factor, denoted as $u : V \to \mathbb{R}$, and $\bar{K}_i$ is the target curvature at the vertex v_i. The length of an edge $[v_i, v_j]$ in terms of u is given by

$$l_{ij} = \exp(u_i)\bar{l}_{ij}\exp(u_j) \tag{6}$$

where $\bar{l}_{ij}$ is the initial edge length. During the flow, we update the triangulation to be Delaunay.

To accelerate the computation, we use Newton's method by solving the Hessian matrix of the discrete Yamabe energy, which is defined as

$$\mathcal{E}(u) = \int^{u} \sum_{i=1}^{n} (\bar{K}_i - K_i) du_i$$

Then the Hessian matrix can be solved as

$$\frac{\partial K_i}{\partial u_j} = \frac{\partial K_j}{\partial u_i} = w_{ij} \tag{7}$$

$$\frac{\partial K_i}{\partial u_i} = -\sum_{[i,j]\in E} w_{ij} \tag{8}$$

where E represents the edge set of the triangulation and w_{ij} is defined in Equations 3 and 4.

3.4. Koebe's Iteration for Topological Poly-annulus

Even though rigorous proof and analysis of the techniques mentioned above have been provided for simply connected domains of arbitrary topology, conformal mapping for multiply connected domains, such as human skull surface, requires additional procedure. Koebe's iteration method [47] provides an elegant approach for genus zero multiply connected surfaces.

Theorem 3 (Koebe) *Suppose (S, g) is a multiply connected annulus with a Riemannian metric g, then there exists a conformal map $\phi : S \to \mathbb{C}$, which maps S to the unit disk with circular holes. Such kind of conformal mappings are unique up to a Möbius transformation [43]. (The proof can be found in [43]).*

4. Computational Algorithms

The skull surface in our case is regarded as a multiply connected region with zero genus and multiple boundaries. Dynamic Yamabe flow is applied to compute the conformal mapping to planar circle domains with Koebe's iteration framework. For registration purpose, we use constrained harmonic mapping to determine the matching between skulls.Figure 2 shows the flowchart of our method.

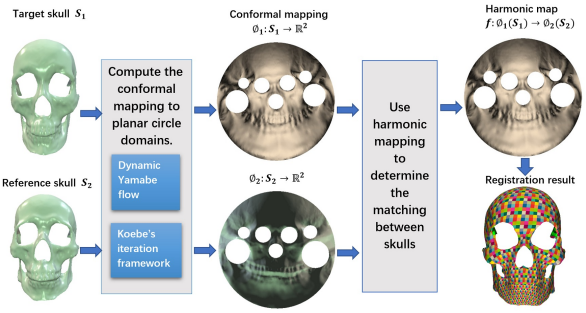

Figure 2: A general flowchart of our method

Algorithm 1: Conformal Mapping on Annulus

Input: The input topological annulus mesh M with boundary $\partial M = \gamma_1 - \gamma_0$,target curvature $\bar{K}$, threshold ϵ

Output: The resulting metric function l_{ij}, and the embedding to canonical annulus

Double cover M to construct M_1, which is close with genus of 1;
Compute the initial edge length $\bar{l}_{ij}$ induced by the the surface embedding in $\mathbb{R}^3$, initialize the conformal factor u to be all zeros;
while *true* **do**
    Compute the edge lengths with Eqn 6;
    Compute corner angles and edge weight as in Eqn 3 and 4;
    Update the triangulation to be Delaunay according to the cotangent edge weight by edge swapping ;
    Compute vertex curvature using Eqn 1;
    if $\forall i, |\bar{K}_i - K_i| < \epsilon$ **then**
        break;
    Compute the gradient of the Ricci flow;
    Compute the Hessian of the Ricci energy with Eqn 7 and 8;
    Solve the linear system $Hess(u)\delta u = \nabla E(u)$;
    $u = u + \delta u$;
end
Compute the edge length $\{l_{ij}\}$;
Cut the surface to remove the double covering to get $\bar{M}$;
Embed $\bar{M}$ on $\mathbb{C}$ equidistantly to make the length of image $\phi(\gamma_1)$ of γ_1 to be 2π;
Map the surface $\phi(\bar{M})$ into a planar annulus with complex exponential map $\exp z$;
return *the metric* $\{l_{ij}\}$ *and the embedding of* $\exp z$

4.1. Dynamic Yamabe Flow on Poly-annulus

Dynamic Yamabe flow on topological disks has been discussed thoroughly [41]. Based on the theoretic correctness

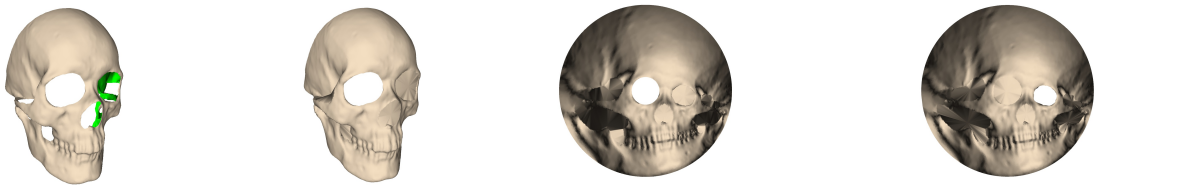

(a) Original mesh with eight boundaries (b) Fill 6 holes (c) Step 1 (d) Fill the first hole and open another

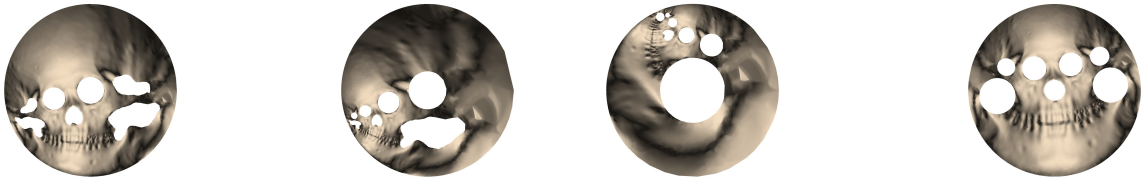

(e) Result after step 2 (f) Result after step 4 (g) Result after step 6 (h) Final result

Figure 3: Demonstration of Koebe's iteration method. (a) is the original surface with eight boundaries. (b) illustrates the hole-filling results. (c) shows the first conformal mapping result from (b) to canonical annulus. (d) closes the first hole and opens the second. (e) is the second conformal mapping result after removing all fillings for better visualization. (f)(g) are results after the step 4 and 6. (h) represents the final result, where all the boundaries are perfect circles.

for arbitrary topology[18], we will generalize the algorithm to topological poly-annulus .

Hole filling and puncturing It is necessary to fill and puncture the holes on skull models so that Koebe's iteration algorithm can be used, as well as that the poly-annulus can be modified to annulus or vice versa. The quality of filling has no effect on the algorithm result. So we will just find the center point of each hole and connect the center point to the vertices on the hole boundary edges to construct triangles. When puncturing, we remove the center points and all the triangles attached to those points.

Dynamic Yamabe flow on Annulus To compute the conformal mapping from topological annulus to canonical planar annulus, we first double cover the annulus [21] to construct a closed surface with genus of 1. Then we can apply the euclidean Ricci flow process to compute the planar metric. Finally, an exponential map on the complex plane will be composed to the planar embedding to get the final mapping to the canonical annulus. The details of the algorithm are shown in Algorithm 1.

4.2. Koebe's Iteration for Poly-annulus

In order to solve the multiply connected region skull surface with boundary and 7 holes conformal mapping, Koebe's iterative framework is used. The basic idea is as follows: first, fill the holes of a skull, open a hole each time to generate a topological annulus with zero genus and two boundaries. Then, calculate the conformal mapping of the annulus to canonical annulus using dynamic Yamabe flow. Repeat this step, each hole is mapped to a circle in turn until all the inner boundaries converge to standard circles. After completing the iterative process, the conformal mapping between multi-connected region with holes and the unit disk with circular holes is obtained.The steps of Koebe's iteration algorithm are stated in Algorithm 2, demonstrated in Figure 3 and the result is in Figure 4. The conformal mapping preserves intrinsic symmetry, hence the final results are symmetric.

Algorithm 2: Generalized Koebe's Iteration for Poly-annulus

Input: Multi-connected surface M with boundaries $\gamma_0, \gamma_1, \gamma_2, \gamma_3, \gamma_4, \gamma_5, \gamma_6, \gamma_7$, threshold ϵ

Output: Conformal mapping $\phi : M \to \bar{M}$, where $\bar{M}$ is planar circle domain with (c_i^0, r_i^0) representing the center and radius for each boundary

Fill all boundaries γ_k with topological disks D_k, $\partial D_k = \gamma_k, k = 1, ..., 7$;

while $\sum_{k=1}^{7} |c_k^{t+1} - c_k^t| + |r_k^{t+1} - r_k^t| > \epsilon$ **do**

  for $k = 1, ..., 7$ **do**

    Remove one disk D_k to construct an annulus S_k;

    Solve for the conformal mapping $\phi : S_k \to \bar{S}_k$ using Algorithm 1;

    Fill the hole on $\bar{S}_k$ with $\bar{D}_k$;

  end

  compute the centers and radii (c_k^{t+1}, r_k^{t+1}) for disks $\bar{D}_k, \forall k$;

end

return ϕ

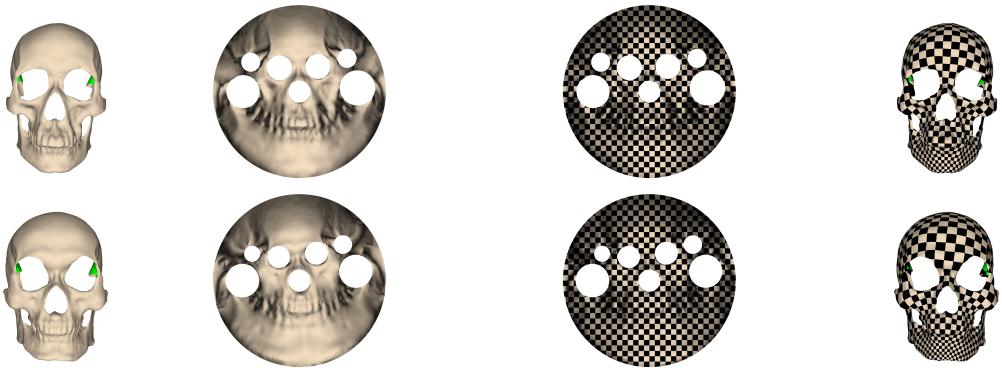

(a) Original skull surface (b) Conformal mapping result (c) Textured with checker board on circle domain (d) Textured with checker board on original surface

Figure 4: The visualized result of conformal mapping on multiply connected surfaces. In column (b) and (c), we can verify that all the inner circles are close to perfect circle. The conformal mapping result is unique up to a Möbius transformation.

4.3. Constrained Harmonic Mapping

In order to find the registration between two surfaces, landmarks are always marked before deformation process begins. Different from human face surfaces, skull surfaces do not have obvious landmarks such as eyebrows, canthus, nose tip, or lips. In our registration process, we use the boundaries of the skull surfaces as intrinsic landmarks. The boundaries are mapped onto circles, and automatically aligned. A constrained harmonic mapping in Algorithm 3 is then applied to the circle domains obtained from the Algorithm 2. Figure 5 shows the mapping between skull surfaces. The resulting maps are conformal diffeomorphic and unique up to a mobius map; the algorithm converges exponentially fast in terms of iterations.

Algorithm 3: Constrained Harmonic Mapping for Circle Domains

Input: Surfaces S_1 and S_2 with boundaries $\{\gamma_i\}$ and $\{\delta_i\}$, along with the circle domain embedding $\phi(S_1)$ and $\phi(S_2)$.

Output: Harmonic mapping $f : \phi(S_1) \to \phi(S_2)$ with boundaries matching

1 Set boundary conditions such that $f(\phi(\gamma_i)) = \phi(\delta_i)$;
2 Solve Poisson Equation with boundary conditions;
3 **return** *the harmonic mapping* f

5. Experimental Result and Evaluation

This research was carried out on a database of whole-head CT scans of volunteers mostly belonging to the Han ethnic group in the North of China. The CT scans were obtained with a clinical multislice CT scanner system (Siemens Sensation16). First, we extracted the craniofacial borders from the original CT slice images and reconstructed the 3D craniofacial meshes with a marching cubes algorithm [28]. We cut away the back part of the craniofacial model because there were too many vertices in the whole head, and the features are mainly concentrated on the front part of the head. One model is randomly chosen as the reference model, while other models are chosen as the target models for registration. The algorithms are implemented using generic C++ under Windows Visual Studio and Matlab. All the experiments are conducted on a personal computer with Core i7-7700 CPU and 8GB Memory.

5.1. Automatic Registration

Figure. 5 shows the process of the registration. The left column shows the source surface, and the right column shows the target surface. Both surfaces are conformally mapped to planar circle domains on the top row, the mappings are denoted as $\varphi_k : S_k \to \mathbb{R}^2$. The two circle domains $\varphi_k(S_k)$ have different configurations, the inner circle centers and radii are not identical. Then we compose a harmonic map $f : \varphi_1(S_1) \to \varphi_2(S_2)$ which maps the inner circles to the corresponding inner circles. The registration result is shown by color encoded texture mapping (e,f), where the corresponding checkers share the same color. The whole computational pipeline is completely automatic, without any manual input or user intervention.

5.2. Global Diffeomorphism

In our method, the multiply connected is conformally mapped onto a planar circle domain with dynamic Yamabe flow; the existence and the uniqueness of the solution are theoretically guaranteed as Theorem 3 stated in paper. Our method can easily achieve global optima and always find the same unique best solution for near-isometric surface.

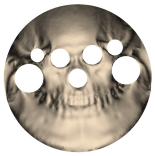

(a) $\phi_1 : S_1 \to \mathbb{R}^2$

(b) Harmonic map $f : \phi_1(S_1) \to \phi_2(S_2)$

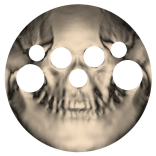

(c) $\phi_2 : S_2 \to \mathbb{R}^2$

(d) Registration result from Koebe's iteration method

(e) Improved Registration result with constrained harmonic mapping

(f) Target surface

Figure 5: Registration result. (a) and (c) are the same as in Figure 4. (b) illustrates the harmonic mapping result, constraining the circle boundaries in (a) to match the circle boundaries in (c). (d) represents the initial registration result targeted at (f). (e) improves the registration results especially in teeth, cheekbone and nose area.

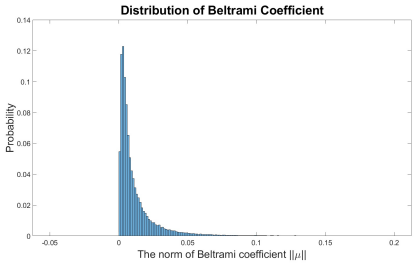

Figure 6: Distribution of Beltrami Coefficients induced by our mapping

In order to verify whether the mapping is globally homeomorphic (injective and surjective), we compute the Beltrami coefficient μ for each face [44, 42]. The mapping is piecewise linear, on each triangular face, the mapping can be locally represented as $w = \alpha z + \beta \bar{z}$, $\alpha, \beta \in \mathbb{C}$. The Beltrami coefficient $\mu = \beta/\alpha$. It can be shown that the mapping is homeomorphic if and only if $\|\mu\| < 1$; the mapping is conformal if and only if $\|\mu\| = 0$. We compute the norm of μ on each face, and show the histogram of the Beltrami coefficient norms as in Figure 6. It is obvious that all the norms of the Beltrami coefficients are less than 1, so the mapping is homeomorphic; the histogram highly concentrates near the 0, less than 1% of faces have Beltrami coefficients $||\mu|| > 0.05$, therefore the mapping is highly conformal. This observation is consistent with the theoretic claim of discrete uniformization.

5.3. Complicated Topology and Robustness

The algorithm to compute holomorphic differential [48], used in Koebe's iteration [47] can collapse for meshes with low qualities, even though the solution does exist theoretically. In contrast, the dynamic Yamabe flow method proposed in this work converges to the unique solution guaranteed by the discrete uniformization theorems [17, 14] and proved using hyperbolic geometry and variational approach in [14]. While the holomorphic 1-form method is equivalent to solve an elliptic partial differential equation on a discrete surface based on Finite Element Method(FEM) [51]. If the triangulation are with low qualities, then the convergence can not be guaranteed to hold. The current method is robust to meshes with low qualities. This theoretic advancement greatly improves the stability and accuracy of the registration.

We design an experiment to demonstrate the capability of the proposed method to handle complex topology. Figure 7 shows the mapping results obtained by the conventional holomorphic differential method [48] (left) and the current method (right). It is clear that holomorphic differential method introduces a large amount of flippings, and fails to produce a parameterization; in contrast, the proposed method can produce globally bijective mapping.

Figure 8 shows the robustness of the proposed method to low quality meshes. Left frame shows a mesh with a large amount of obtuse angles, which produces discrete Laplacian matrix with high condition number; conventional methods [20, 15] fails to produce sensible mapping. Whereas our proposed method achieves global homeomorphic mapping, shown in the right frame.

5.4. Registration Accuracy

Figure 5 and 9 show our registration results. The correspondences of two registered skulls are shown by color encoding. Each checker on the source is mapped to a checker

(a) Mapping Result using holomorphic 1-form [48] (b) Our mapping Result using dynamic Yamabe flow

Figure 7: The comparison of using (a)holomorphic 1-form and (b)dynamic Yamabe flow. The result from holomorphic 1-form has overwhelming number of face flips due to the undesirable triangulation quality. The low quality triangulation has minor effects on the dynamic Yamabe flow.

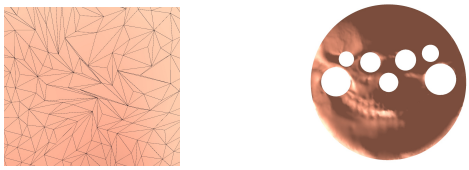

(a) An enlarged view of poor quality triangles (b) Conformal mapping result of our method

Figure 8: Robustness. (a)Even dense models(50k vertices) can have poor quality triangles. However, (b) shows that our method is able to robustly construct good mapping results.

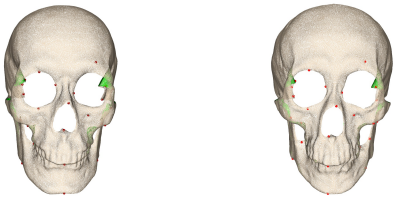

(a) Feature points (b) Corresponding points

Figure 9: Registration results visualized with feature points correspondence. (a) shows the feature points labeled by craniofacial experts. (b) presents the corresponding points from our registration results.

on the target with the same color. In order to measure the registration accuracy, we manually select 16 anatomic feature points on the source and target. Then we measure the distance between the image of a feature point and the corresponding feature point on the target, and normalized by the diagonal of the bounding box of the skull surface.

We have conducted the experiments with our method on 105 skulls in the database. Most non-rigid registration methods require manually labelled feature points and can

Table 1: Average error comparison of our method and ICP

Skull Numbers	Average Error of our method	Average Error of ICP	Registration improvement
105	2.2489%	2.5812%	0.3323%

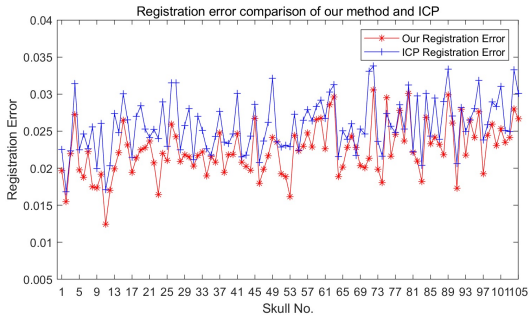

Figure 10: Error comparison of our method and ICP

not be realized automatically; the previous conformal parameterization method may fail on some skulls whereas our method can achieve high registration accuracy because it is quite different from the existing conformal mapping methods [9, 31, 41, 47, 48](details can be found in supplementary materials). Here we compared our method only with classic automatic ICP method, the registration error results are showed in Table 1. and Figure 10. The results show that our average error is less than ICP average error.

6. Conclusions

This work proposes a novel method for skull surface registration based on discrete uniformization theory, which can handle surfaces with complicated topologies and low mesh qualities. The multiply connected skull surface is conformally mapped onto a planar circle domain, the existence and the uniqueness of the solution are theoretically guaranteed. Our experimental results show that the method is fully automatic without user intervention, robust to low quality meshes, achieves global diffeomorphism and high registration accuracy. The proposed method can be directly generalized to register different shapes with complicated topologies as well. In the future, we will explore further for partial skull surface matching applying the similar method.

Acknowledgements

This work was supported by Natural Science Foundation (Grant No. 176228, No. 141855, No.1737812) and the National Natural Science Foundation of China (Grant No. 61702293, No.61772105, No.61720106005, No.61432003, No.61572078) and China Postdoctoral Science Foundation No. 2017M622137.

References

[1] Neşe Alyuz, Berk Gokberk, and Lale Akarun. Regional registration for expression resistant 3-d face recognition. *IEEE Transactions on Information Forensics and Security*, 5(3):425–440, 2010.

[2] Paul J Besl and Neil D McKay. Method for registration of 3-d shapes. In *Sensor Fusion IV: Control Paradigms and Data Structures*, volume 1611, pages 586–607. International Society for Optics and Photonics, 1992.

[3] Fred L. Bookstein. Principal warps: Thin-plate splines and the decomposition of deformations. *IEEE Transactions on pattern analysis and machine intelligence*, 11(6):567–585, 1989.

[4] Benedict J Brown and Szymon Rusinkiewicz. Non-rigid range-scan alignment using thin-plate splines. In *3D Data Processing, Visualization and Transmission, 2004. 3DPVT 2004. Proceedings. 2nd International Symposium on*, pages 759–765. IEEE, 2004.

[5] Benedict J Brown and Szymon Rusinkiewicz. Global non-rigid alignment of 3-d scans. In *ACM Transactions on Graphics (TOG)*, volume 26, page 21. ACM, 2007.

[6] Francis E Burstall, Dirk Ferus, Katrin Leschke, Franz Pedit, and Ulrich Pinkall. *Conformal geometry of surfaces in S4 and quaternions*. Springer, 2004.

[7] Yucong Chen, Junli Zhao, Qingqiong Deng, and Fuqing Duan. 3d craniofacial registration using thin-plate spline transform and cylindrical surface projection. *PloS one*, 12(10):e0185567, 2017.

[8] Tianyu Cheng, Juping Gu, Liang Hua, XinSong Zhang, Hui Yang, Junhong Li, and Yiming Xu. Three-dimensional skull registration based on clifford algebra pupil distance invariability and visualization platform building. In *2017 Chinese Automation Congress (CAC)*, pages 7871–7875. IEEE, 2017.

[9] Kiran Chilakamarri, Nathaniel Dean, and Michael Littman. Three-dimensional tutte embedding. *Congressus Numerantium*, pages 129–140, 1995.

[10] Bennett Chow. The ricci flow on the 2-sphere. *Journal of Differential Geometry*, 33(2):325–334, 1991.

[11] Haili Chui and Anand Rangarajan. A new point matching algorithm for non-rigid registration. *Computer Vision and Image Understanding*, 89(2-3):114–141, 2003.

[12] Junei Dai, Xianfeng David Gu, and Feng Luo. *Variational principles for discrete surfaces*, volume 4. International Pressof Boston Incorporated, 2008.

[13] Qingqiong Deng, Mingquan Zhou, Wuyang Shui, Zhongke Wu, Yuan Ji, and Ruyi Bai. A novel skull registration based on global and local deformations for craniofacial reconstruction. *Forensic science international*, 208(1-3):95–102, 2011.

[14] Xianfeng Gu, Ren Guo, Feng Luo, Jian Sun, Tianqi Wu, et al. A discrete uniformization theorem for polyhedral surfaces ii. *Journal of Differential Geometry*, 109(3):431–466, 2018.

[15] Xianfeng Gu, Sen Wang, Junho Kim, Yun Zeng, Yang Wang, Hong Qin, and Dimitris Samaras. Ricci flow for 3d shape analysis. In *Computer Vision, 2007. ICCV 2007. IEEE 11th International Conference on*, pages 1–8. IEEE, 2007.

[16] Xianfeng Gu, Yalin Wang, Tony F Chan, Paul M Thompson, and Shing-Tung Yau. Genus zero surface conformal mapping and its application to brain surface mapping. *IEEE transactions on medical imaging*, 23(8):949–958, 2004.

[17] Xianfeng David Gu, Feng Luo, Jian Sun, Tianqi Wu, et al. A discrete uniformization theorem for polyhedral surfaces. *Journal of Differential Geometry*, 109(2):223–256, 2018.

[18] Xianfeng David Gu and Shing-Tung Yau. *Computational conformal geometry*. International Press Somerville, Mass, USA, 2008.

[19] Richard S Hamilton. Three-manifolds with positive ricci curvature. *Journal of Differential Geometry*, 17(2):255–306, 1982.

[20] Richard S Hamilton. The ricci flow on surfaces. In *Mathematics and general relativity, Proceedings of the AMS-IMS-SIAM Joint Summer Research Conference in the Mathematical Sciences on Mathematics in General Relativity, Univ. of California, Santa Cruz, California, 1986*, pages 237–262. Amer. Math. Soc., 1988.

[21] Wei Hong, Xianfeng Gu, Feng Qiu, Miao Jin, and Arie Kaufman. Conformal virtual colon flattening. In *Proceedings of the 2006 ACM symposium on Solid and physical modeling*, pages 85–93. ACM, 2006.

[22] Yongli Hu, Mingquan Zhou, and Zhongke Wu. A dense point-to-point alignment method for realistic 3d face morphing and animation. *International Journal of Computer Games Technology*, 2009:3, 2009.

[23] Tim J Hutton, Bernard F Buxton, and Peter Hammond. Automated registration of 3d faces using dense surface models. In *BMVC*, pages 1–10. Citeseer, 2003.

[24] Miao Jin, Junho Kim, and Xianfeng David Gu. Discrete surface ricci flow: Theory and applications. In *IMA International Conference on Mathematics of Surfaces*, pages 209–232. Springer, 2007.

[25] Miao Jin, Junho Kim, Feng Luo, and Xianfeng Gu. Discrete surface ricci flow. *IEEE Transactions on Visualization and Computer Graphics*, 14(5):1030–1043, 2008.

[26] Lili Ju, Josh Stern, Kelly Rehm, Kirt Schaper, Monica Hurdal, and David Rottenberg. Cortical surface flattening using least square conformal mapping with minimal metric distortion. In *Biomedical Imaging: Nano to Macro, 2004. IEEE International Symposium on*, pages 77–80. IEEE, 2004.

[27] Bruno Lévy, Sylvain Petitjean, Nicolas Ray, and Jérome Maillot. Least squares conformal maps for automatic texture atlas generation. In *ACM transactions on graphics (TOG)*, volume 21, pages 362–371. ACM, 2002.

[28] William E Lorensen and Harvey E Cline. Marching cubes: A high resolution 3d surface construction algorithm. In *ACM siggraph computer graphics*, volume 21, pages 163–169. ACM, 1987.

[29] Lok Ming Lui, Sheshadri Thiruvenkadam, Yalin Wang, Paul M Thompson, and Tony F Chan. Optimized conformal surface registration with shape-based landmark matching. *SIAM Journal on Imaging Sciences*, 3(1):52–78, 2010.

[30] Feng Luo. Rigidity of polyhedral surfaces. *arXiv preprint math/0612714*, 2006.

[31] TC Ng, Xianfeng Gu, and LM Lui. Teichmüller extremal map of multiply-connected domains using beltrami holomorphic flow. *Journal of Scientific Computing*, 60(2):249–275, 2014.

[32] Wenyu Qin, Yongli Hu, Yanfeng Sun, and Baocai Yin. An automatic multi-sample 3d face registration method based on thin plate spline and deformable model. In *Multimedia and Expo Workshops (ICMEW), 2012 IEEE International Conference on*, pages 453–458. IEEE, 2012.

[33] Szymon Rusinkiewicz and Marc Levoy. Efficient variants of the icp algorithm. In *3D Digital Imaging and Modeling, 2001. Proceedings. Third International Conference on*, pages 145–152. IEEE, 2001.

[34] David C Schneider and Peter Eisert. Algorithms for automatic and robust registration of 3d head scans. *JVRB-Journal of Virtual Reality and Broadcasting*, 7(7), 2010.

[35] Rui Shi, Wei Zeng, Zhengyu Su, Hanna Damasio, Zhonglin Lu, Yalin Wang, Shing-Tung Yau, and Xianfeng Gu. Hyperbolic harmonic mapping for constrained brain surface registration. In *Proceedings of the IEEE Conference on computer vision and pattern recognition*, pages 2531–2538, 2013.

[36] Kehua Su, Li Cui, Kun Qian, Na Lei, Junwei Zhang, Min Zhang, and Xianfeng David Gu. Area-preserving mesh parameterization for poly-annulus surfaces based on optimal mass transportation. *Computer Aided Geometric Design*, 46:76–91, 2016.

[37] Sen Wang, Yang Wang, Miao Jin, Xianfeng David Gu, and Dimitris Samaras. Conformal geometry and its applications on 3d shape matching, recognition, and stitching. *IEEE Transactions on Pattern Analysis & Machine Intelligence*, (7):1209–1220, 2007.

[38] Yang Wang, Mohit Gupta, Song Zhang, Sen Wang, Xianfeng Gu, Dimitris Samaras, and Peisen Huang. High resolution tracking of non-rigid motion of densely sampled 3d data using harmonic maps. *International Journal of Computer Vision*, 76(3):283–300, 2008.

[39] Caroline Wilkinson. Computerized forensic facial reconstruction. *Forensic Science, Medicine, and Pathology*, 1(3):173–177, 2005.

[40] Jiaolong Yang, Hongdong Li, and Yunde Jia. Go-icp: Solving 3d registration efficiently and globally optimally. In *Proceedings of the IEEE International Conference on Computer Vision*, pages 1457–1464, 2013.

[41] Xiaokang Yu, Na Lei, Yalin Wang, and Xianfeng Gu. Intrinsic 3d dynamic surface tracking based on dynamic ricci flow and teichmüller map. In *Proceedings. IEEE International Conference on Computer Vision*, volume 2017, pages 5400–5408. NIH Public Access, 2017.

[42] Wei Zeng and Xianfeng David Gu. Registration for 3d surfaces with large deformations using quasi-conformal curvature flow. In *Computer Vision and Pattern Recognition (CVPR), 2011 IEEE Conference on*, pages 2457–2464. IEEE, 2011.

[43] Wei Zeng, Lok Ming Lui, Xianfeng Gu, and Shing-Tung Yau. Shape analysis by conformal modules. *Methods and Applications of Analysis*, 15(4):539–556, 2008.

[44] Wei Zeng, Joseph Marino, Krishna Chaitanya Gurijala, Xianfeng Gu, and Arie Kaufman. Supine and prone colon registration using quasi-conformal mapping. *IEEE Transactions on Visualization and Computer Graphics*, 16(6):1348, 2010.

[45] Wei Zeng, Dimitris Samaras, and David Gu. Ricci flow for 3d shape analysis. *IEEE Transactions on Pattern Analysis and Machine Intelligence*, 32(4):662–677, 2010.

[46] Wei Zeng, Xiaotian Yin, Yun Zeng, Yukun Lai, Xianfeng Gu, and Dimitris Samaras. 3d face matching and registration based on hyperbolic ricci flow. In *Computer Vision and Pattern Recognition Workshops, 2008. CVPRW'08. IEEE Computer Society Conference on*, pages 1–8. IEEE, 2008.

[47] Wei Zeng, Xiaotian Yin, Min Zhang, Feng Luo, and Xianfeng Gu. Generalized koebe's method for conformal mapping multiply connected domains. In *2009 SIAM/ACM Joint Conference on Geometric and Physical Modeling*, pages 89–100. ACM, 2009.

[48] Wei Zeng, Yun Zeng, Yang Wang, Xiaotian Yin, Xianfeng Gu, and Dimitris Samaras. 3d non-rigid surface matching and registration based on holomorphic differentials. In *European Conference on Computer Vision*, pages 1–14. Springer, 2008.

[49] Min Zhang, Yinghua Li, Wei Zeng, and Xianfeng Gu. Canonical conformal mapping for high genus surfaces with boundaries. *Computers & Graphics*, 36(5):417–426, 2012.

[50] Xiaopeng Zheng, Chengfeng Wen, Na Lei, Ming Ma, and Xianfeng Gu. Surface registration via foliation. In *Proceedings of the IEEE Conference on Computer Vision and Pa ern Recognition*, pages 938–947, 2017.

[51] Olgierd Cecil Zienkiewicz, Robert Leroy Taylor, Perumal Nithiarasu, and JZ Zhu. *The finite element method*, volume 3. McGraw-hill London, 1977.